



CA9700367

## RFQ COLD MODEL STUDIES

P. G. Bricault, D. Joffe and H. R. Schneider, TRIUMF, 4004 Wesbrook Mall, Vancouver, B. C., Canada, V6T 2A3

A post accelerator, primarily to provide beams of interest to nuclear astrophysics users, is included in the upgrading and expansion of the **radioactive beam** facility at **TRIUMF**. Singly charged **ion beams**, with  $A \leq 30$ , delivered from the on line **mass separator** with an energy of 2 keV/u, will be accelerated in a stage linac consisting of an RFQ and a post-stripper drift-tube. As a consequence of the low charge-to-mass ratio of the ions, a low operating frequency for the RFQ is required to achieve adequate transverse focusing. **CW operation** is specified to preserve beam intensity. Because of its relatively high specific shunt impedance, mechanical stability, and the absence of vane voltage asymmetries in the end regions, the split-ring 4-rod RFQ structure has been chosen. Several cold models have been built to study three different types of split-ring RFQ structures. Specific shunt impedance and longitudinal **field** have been measured. A comparison of these measurements for various split-ring structures is presented.

### I. INTRODUCTION

A radioactive beam facility based on the ISOL method with a post accelerator was proposed at TRIUMF in 1985 [1]. Two years ago a new study of the post accelerator was started. The specifications dictated primarily by the nuclear astrophysics interests, required a maximum energy of 1.5 MeV/u for ion beams with  $A \leq 30$ .

The acceleration of ions with small charge to mass ratio requires a **low frequency** RFQ. At low frequency the size of the conventional 4-vane RFQ tank becomes very large. To reduce the size of the cavity diameter for frequencies less than 200 MHz, the 4-vane structures are replaced by a form of 4-rod structure in which the quadrupole electrodes (rods) are part of a resonant circuit consisting of a combination of lumped and distributed inductances and capacitances. Two basic type of 4-rod structure have been reported in the literature, viz. the stem supported 0-mode 4-rod structure [5,7], and the split-coaxial structure[2,3,4]. A unit cell of the later may be viewed as two end-to-end  $\lambda/4$  coaxial lines with orthogonal rod pairs interleaved to form the quadrupole electrode geometry. The distributed inter-electrode capacitance and rod inductance determine the structure resonant frequency. In a unit cell of a stem supported structure on the other hand, the two stems for the two rod pairs form the inductance that resonates with the inter-electrode capacitance.

Since the unstable ion beams are produced continuously in the ISOL target-ion source, operation of the RFQ in cw mode is desirable to preserve beam intensity. To avoid high power dissipation concomitant potential structure distortion, an efficient, i.e., high shunt impedance, RFQ structure is then required. With the exception of a 33 MHz RFQ at the University of Kyoto[6], no other low frequency RFQ operating in cw mode has been reported. To address our

needs therefore, a development program was undertaken at TRIUMF.

### II. MODEL DESIGN

According to the beam dynamics the ISAC-1's RFQ will be 8.2 m long, and assuming a power dissipation of 15 kW per meter, the value of the shunt impedance should be larger than 300 k $\Omega$ m. Since the RFQ is very long it will be suitable to select among candidates RFQ one that can be built into several modules. The alignment of the rods in each individual module can be done much easily before insertion of the structure into the tank. In order to do so it is easier if the longitudinal current on the rods presents nulls located at the same position on all the four rods. The current passing through the contact will be negligible. This is the case for the split-coaxial RFQ, the nulls are located are the point where the vanes (or rods) are suspended. In the "0-mode RFQ structure" the surface current is largely confine in the "U" shaped support structures, and are theoretically zero on the rods at the symmetry points between support structures. To optimize the shunt impedance of the later, the supports are equally spaced and then the nulls are not any longer located at the same longitudinal position along the RFQ. This was observed by measuring a voltage unbalance between each rod and the end-plate. We have observed that the voltage asymmetry depends on the separation between the rod's supports.

After many attempts we found that the split-ring RFQ has a very small voltage asymmetry in the end region. In this structure the separation between the stems is much smaller than in the conventional two-stem RFQ structure. Furthermore, the split-ring 4-rod RFQ structure has been chosen, because of its relatively high specific shunt impedance and mechanical stability. The models were made from copper, and a modular assembly technique was used in order to take advantage of the same electrodes, tank and the main ring. Table 1 gives the basic dimensions of the 4-rod split-ring RFQ. The top quarters of the rings were removable, and there were three sets of rod's supports that could be attached to the structure to examine the effects of the different configurations. These three split-ring shapes are labeled RFQ\_1, RFQ\_2 and RFQ\_3. Figure 1 shows the three types of RFQ and fig 2 shows the detail of the rod's attachment in the central region.

Table 1- Dimensions of the 4 rod split-ring RFQ cold models.

R (cm)	8.811
r (cm)	0.952
z (cm)	2.54
S (cm)	2.54
D <sub>rod</sub> (mm)	4.763
R <sub>0</sub> (mm)	2.381
Shape	Rectangular
Diameter (cm)	27.5

Table 2 summarizes the results for those three types of split-ring 4-rod RFQ. The number of modules, the total RFQ's length, frequency, Q value and shunt resistance.

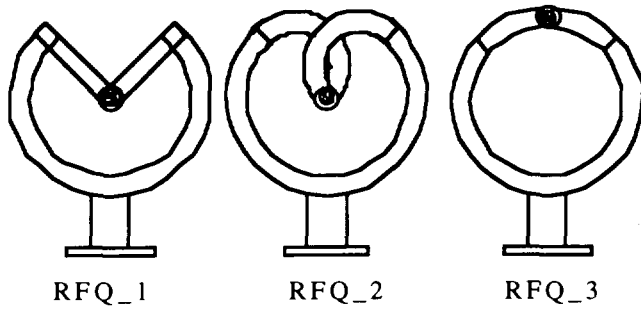


Fig. 1 - Schematic drawing of the 4-rod split-ring RFQ.

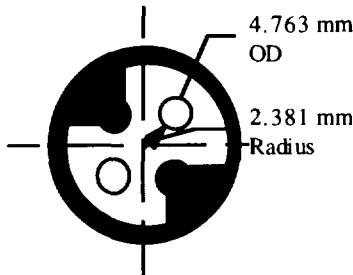


Fig. 2 - Central region of the split-ring 4-rod RFQ.

Table 2 summarize the results obtained for the cold models.

Table 2 - Results of the measurements on the split-ring 4-rod RFQ cold models

Type	# module	L mm	f MHz	Q	$R_s$ k $\Omega$ ·m
RFQ_1	1	191	77.860	3140	49.6
RFQ_1	5	953	78.244	3040	50.3
RFQ_2	1	191	68.738	3390	56.3
RFQ_2	5	953	67.639	2930	56.4
RFQ_3	1	185	75.150	3372	49.4
RFQ_3	3	572	71.587	3232	69.4

The poor Q-value can be explained by the use of a modular assembly technique chosen to spare machining.

### III. ELECTRIC FIELD MEASUREMENTS

#### A Voltage and phase measurement

The voltage and the phase on each individual rod were measured using a Hewlett Packard vector voltmeter with a Hewlett Packard network analyzer as the rf source.

The split-ring 4-rod RFQ has the advantage that the separation between the rod supports is very small. For this reason the voltages on each pair of rods are nearly equal. We also verify that this RFQ has a pure quadrupole mode. Table 4 shows the results of the cold model measurements of the RFQ structure.

Table 4 - Phase and voltage measurement

Ring radius (mm)		88.11			
Ring width (mm)		25.			
Tip radius (mm)		2.38			
Bore radius (mm)		2.38			
Number of modules		3			
Separation between modules		19.05			
RFQ length (mm)		571.5			
Probe #	$\Delta\Phi$ (Deg.)	$\Delta V$ (Volts)	Probe #	$\Delta\Phi$ (Deg.)	$\Delta V$ (Volts)
1A	110.6	6.56	1B	110.4	6.97
2A	-69.2	7.08	2B	-69.2	6.52
3A	110.6	6.51	3B	110.5	6.53
4A	-69.3	7.07	4B	-69.2	6.59

$\Delta\Phi$  is the phase difference between the reference signal and the probes. The phase on probes 1-3 and 2-4 should be the same.  $\Delta V$  is the voltage difference between the vane and the end plate located at ground potential. Here we can see the voltage asymmetry between electrodes 1 - 3 and 2 - 4 is very small. For the split-ring type RFQ the phases on electrodes 1-3 and 2-4 are very close. Also, the phases and the voltages are the same at each end of the rod.

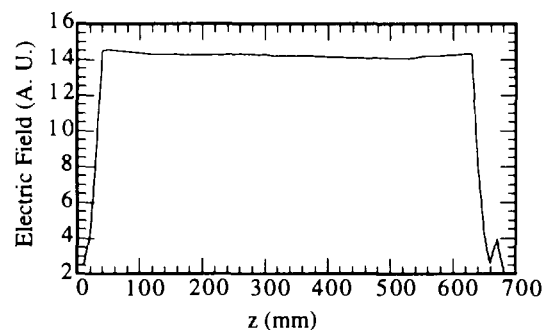


Fig. 3 - Field distribution along the RFQ.

#### B Electric field distribution

The electric field distribution along the RFQ was measured using the bead-pull technique. The bead was placed between the RFQ electrodes and pulled along the RFQ axis by a computer controlled stepping motor. The frequency shift was measured at each step from which the field strengths were calculated. Figure 3 shows the electric field obtained with the three modules connected to each other.

### IV. MODULE LENGTH

Using the cold model RFQ\_3 the module length was varied from 10 cm to 20 cm in order to find the optimum value for the specific shunt impedance,  $R_s = V_p^2 / (2P/l)$ , where  $V_p$  is the peak voltage difference between two electrodes and  $P/l$  the power loss per unit of length. Figure 4 shows the scaled shunt impedance as a function of the separation between two adjacent split-rings. The solid line is a plot of the calculated shunt impedance using the expression for the q value and the shunt impedance,

$$R_S = \frac{L}{R_{Total} C_T},$$

where,

$$R_{Total} = \frac{1}{\sigma \delta} \left( \frac{l_{in}}{2r+z} + \frac{L_{Mod}}{12\pi D_{Rod}} \right) \text{ and}$$

$$C_T = C_T + C_0/L_{Mod},$$

where,  $C_T$  is the capacitance per unit length and  $C_0$  the residual capacitance of one module.  $z$  is the ring width,  $2r$  is the radial width of the ring,  $l_{in}$  is the length of the inner surface of the ring and  $D_{ROD}$  is the rod diameter. The inductance is expressed using a formula for the self inductance of a ring with rectangular cross section,

$$L = N 4\pi R \left[ \frac{1}{2} \left\{ 1 + \frac{1}{6} \left( \frac{r}{R} \right)^2 \right\} \ln 8 / \left( \frac{r}{R} \right)^2 - 0.03 + 0.04 \left( \frac{r}{R} \right)^2 \right]$$

where,  $r/R$  is the ration of the minor to major radius, and  $N$  is a normalization factor deduced from a fit of the measured inductances of various split-ring models. For RFQ\_3 model  $N$  is equal to 0.61.

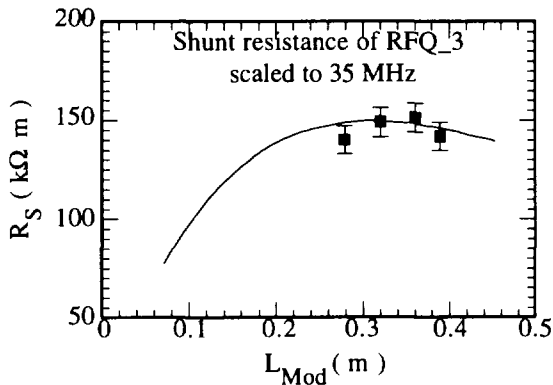


Fig. 4 - Scaled shunt impedance to 35 MHz as a function of the separation between two split-rings.

The shunt impedance shows a broad peak centered around 35 cm. Simulations using MAFIA give a similar value [8].

## VI. NEW SPLIT-RING RFQ COLD MODEL

A new cold model split-ring 4-rod RFQ based on the results of the MAFIA simulation, was built, see Fig. 5. The dimensions were optimized for the best shunt resistance. Table 5 gives the dimensions of the structure and also the shunt resistance, phases and voltages between the end plate and the rods.

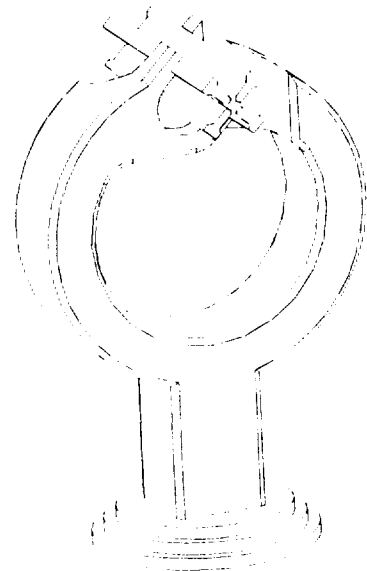


Fig. 5- Scaled cold model of the new split-ring 4-rod RFQ.

Table 6 - Phase and voltage measurement of the split-ring 4-rod RFQ.

Ring radius (mm)	150	
Ring width (mm)	70	
Tip radius (mm)	3.5	
Bore radius (mm)	3.5	
Number of module	1	
Separation between module (mm)	175	
RFQ length (mm)	175	
Frequency (MHz)	64.9475	
Shunt Resistance(35MHz) ( kΩ•m)	282.	
Probe no	ΔΦ( Deg. )	ΔV( Volts )
1	71.0	11.9
2	-109.4	13.3
3	70.9	12.2
4	-107.7	13.1

## Reference

- [1] G. E. McMicheal, B. G. Chidley and R. M. Hutcheon, AECL 8960/TRI-DN-85-3.
- [2] R. W. Müller, "Layout of a High Intensity Linac for Very Heavy Ions with RFQ focusing", GSI-REP-79-7.
- [3] S. Arai et al. IEEE 1991 Particle Accelerator Conf.
- [4] R. W. Müller, U. Kopf, J. Bolle, S. Arai, P. Spädtke, Proceeding of the 1984 International Conference on Linear Accelerator, p. 77.
- [5] A. Schempp et al. Nucl. Instr. & Meth. B10/11 (1985) p. 831.
- [6] H. Fujisawa et al. Bulletin of Institute for Chemical Research, Kyoto University, vol. 70, no 1, 1992.
- [7] A. Schempp et al. Nucl. Instr. & Meth. A278 (1989) p. 766.
- [8] P. G. Bricault, D. Joffe and H. R. Schneider, "Simulation of the TRIUMF split-ring 4-rod RFQ with MAFIA", this conference.